PHYSICAL REVIEW B VOLUME 24, NUMBER 8 15 OCTOBER 1981

Optical properties of cesium tetracyanoquinodimethanide, $Cs_2(TCNQ)_3$

K. D. Cummings and D. B. Tanner
Department of Physics, The Ohio State University, Columbus, Ohio 43210

Joel S. Miller
Occidental Research Corporation, Irvine, California 92713

(Received 2 April 1981)

Room-temperature polarized reflectance measurements have been made on cesium tetracyanoquinodimethanide, $Cs_2(TCNQ)_3$, over the frequency range between the far infrared and the near ultraviolet. The optical properties of the compound were obtained by Kramers-Kronig analysis. These properties are dominated by vibrational features at low frequencies and by electronic excitations at high frequencies. The observed vibrational features include ordinary intramolecular modes and "anomalous" infrared activity of the totally symmetric vibrations. This latter absorption results from the interaction of these vibrations with the unpaired electron on the $TCNQ^-$ ion. Two electronic excitations are observed for the electric field polarized along the TCNQ chains. The excitation higher in frequency is attributed to an intermolecular charge transfer from one $TCNQ^-$ ion to an adjacent ion, while the lower-frequency excitation results from a charge-transfer transition to an adjacent neutral molecule. Estimates for the effective on-site Coulomb repulsion energy U of 1.14 eV, and for the transfer matrix element t of 0.17 eV, are obtained from these data. Experimental values for the electron-molecular-vibration coupling constants are also obtained.

I. INTRODUCTION

This paper describes the results of a study of the optical properties of cesium tetracyanoquinodimethanide, $Cs_2(TCNQ)_3$. We have measured the room-temperature polarized reflectance of single crystals of $Cs_2(TCNQ)_3$ over the frequency range between the far infrared and the near ultraviolet. The optical properties have been obtained by Kramers-Kronig analysis of the reflectance.

The electronic properties of radical-ion organic solids, such as $Cs_2(TCNQ)_3$, are determined by the relative importance of three basic interactions of the unpaired electrons of the ions. These interactions are the overlap of the electronic wave function between sites, the Coulomb repulsive interaction between two electrons on the same or adjacent sites, and the interaction of the electron with phonons (both lattice vibrations and intramolecular modes of the molecule). Optical data can be used to measure the strengths of these interactions.

$Cs_2(TCNQ)_3$ is a complex TCNQ salt by virtue of its 2:3 stoichiometry. The crystal structure, determined by Fritchie and Arthur,[1] consists of chains of TCNQ molecules and Cs^+ ions along the b axis. In the TCNQ chain, the bond lengths indicate that pairs or dimers of $TCNQ^-$ ions are placed between $TCNQ^0$ neutral molecules. The basic formula unit then consists of two ions and one neutral molecule. The [100] and [001] projections of this structure are shown in Fig. 1.

The room-temperature dc conductivity[2–5] of $Cs_2(TCNQ)_3$, $\sim 10^{-3}\ \Omega^{-1}\,cm^{-1}$, is intermediate between the highly insulating 1:1 TCNQ salts such as K-TCNQ and the "metallic" compounds such as TTF-TCNQ (where TTF stands for tetrathiofulvalene). The temperature dependence of the con-

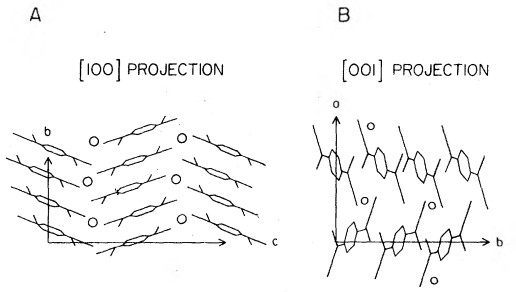

FIG. 1. [001] and [100] projections of the $Cs_2(TCNQ)_3$ structure. The small circles are Cs atoms with the TCNQ molecules stacked in between.

ductivity is characteristic of a semiconductor with a full energy gap of 0.72 eV. Magnetic measurements[6] yield a smaller estimate for the gap of 0.1 eV.

The optical properties of $Cs_2(TCNQ)_3$ have been studied several times previously.[7–17] The first measurements were by Iida,[7] who made unpolarized measurements above 0.5 eV and interpreted the results in terms of charge-transfer excitations dominated by Coulomb repulsion. Electronic transitions have been studied by a number of workers[8–13] since Iida. Polarized reflectance measurements to study vibrational modes in $Cs_2(TCNQ)_3$ have been made by Belousov *et al.*[14] between 0.05 eV (400 cm^{-1}) and 0.6 eV (5000 cm^{-1}). Other infrared measurements have been made by Kondow and Sakata,[15] Girlando *et al.*,[16] and Khursandova *et al.*[17]

Despite this significant amount of work, we have made comprehensive measurements of the optical properties of $Cs_2(TCNQ)_3$. This work was motivated by a number of reasons: First, there has been no work in the far infrared (below 400 cm^{-1}); there has been no comprehensive study using polarized light spanning the vibrational and electronic excitation regions, and many of the previous studies stopped near 0.5 eV where we find an absorption maximum. Second, the structure of $Cs_2(TCNQ)_3$, consisting as it does of linear chains of dimers spaced by neutral molecules, makes this work a companion piece to earlier studies[18] of $D(CH_3)Fc$-TCNQ [$D(CH_3)Fc$ stands for decamethylferrocinium; this system contains isolated dimers] and [19,20]K-TCNQ (a linear chain of interacting dimers). Third, we were interested in comparing the optical properties of $Cs_2(TCNQ)_3$ with those of $N(CH_3)_3H$-I-TCNQ.[21] Both compounds have an average charge per TCNQ molecule of $2e/3$; in $Cs_2(TCNQ)_3$ the molecules are not uniformly spaced along the chain while in $N(CH_3)_3H$-I-TCNQ they are uniformly spaced. These structural differences have profound effects on the optical properties.

The next section of the paper describes sample preparation and optical techniques while the third section presents our reflectance data and the results of the Kramers-Kronig analysis. In the final section, we discuss the electronic transitions and the vibrational features that we observe.

II. EXPERIMENTAL TECHNIQUES

The 2:3 $Cs_2(TCNQ)_3$ was prepared by the method of Melby *et al.*[22] Ultrapure cesium iodide (Alfa) and gradient sublimed 7,7,8,8-tetracyano-*p*-quinodimethane were mixed in a 1:1 ratio in suitably pure hot acetonitrile.[22] The hot intense green solution was sealed and placed in a preheated Dewar which slowly equibrated with ambient temperature. After two weeks the product was collected by filtration and air dried. Large well-formed crystals suitable for optical studies were prepared by this technique.

The room-temperature polarized reflectance of $Cs_2(TCNQ)_3$ crystals was measured using two instruments. Between 700 and 30 000 cm^{-1} (0.09–3.37 eV) we used a vacuum spectrometer built around a Perkin-Elmer model 16U grating monochromator. Figure 2 is a diagram of this spectrometer. The entire spectrometer can be evacuated to pressures below 1 Torr to reduce the absorption by atmospheric water vapor in the infrared region. All surfaces within the vacuum box were covered with 3M Nextel® flat black paint to reduce stray light. Three sources, four gratings, and three detectors were used to cover the infrared, visible, and near ultraviolet regions with moderate resolution, $\Delta\omega/\omega \sim 10^{-3}$. Long-pass and bandpass filters eliminated unwanted orders of diffraction. A large spherical mirror imaged the exit slit of the monochromator onto a single crystal mounted in the sample holder. A second spherical mirror focused the reflected light onto the detector. The detector was a thermocouple below 4000 cm^{-1} (0.5 eV) with a glowbar source, a PbS photoconductor between 4000 and 15 000 cm^{-1} (0.5–1.9 eV) with a tungsten lamp source and a photomultiplier above 15 000 cm^{-1} with either the tungsten source or a deuterium lamp source. The tungsten source was used up to 27 000 cm^{-1} (3.3 eV) and a deuterium lamp was used at higher frequencies. In the middle infrared a wire grid polarizer was utilized while dichroic polarizers were used in the near infrared through ultraviolet regions.

Below 700 cm^{-1} (0.09 eV) a Michelson interferometer, diagrammed in Fig. 3, was used to measure the polarized reflectance of a mosaic of $Cs_2(TCNQ)_3$ crystals. The interferometer and its operation have been described previously.[23] However, an assembly has been added to allow polarized reflection measurements. With four different thicknesses of Mylar for beam splitters, a frequency region from 10 to 700 cm^{-1} (0.002–0.09 eV) was examined with a resolution of $\Delta\omega/\omega \sim 10^{-2}$. A wire grid polarizer was used throughout this region. An accurate absolute value for the reflectance was obtained by comparing the reflectance

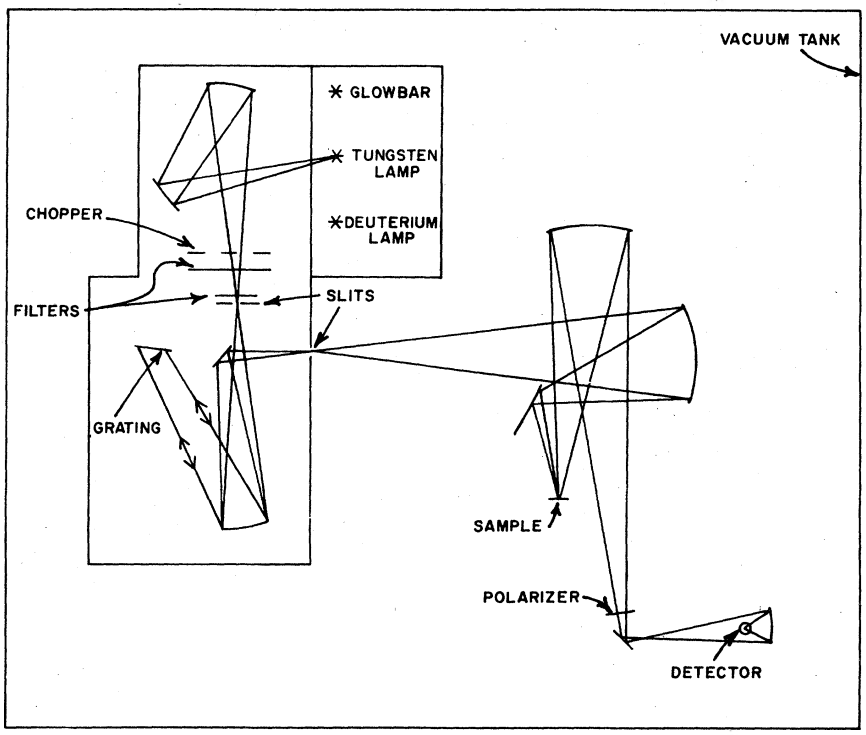

FIG. 2. Diagram of grating spectrometer used to cover the 700—30 000 cm^{-1} region.

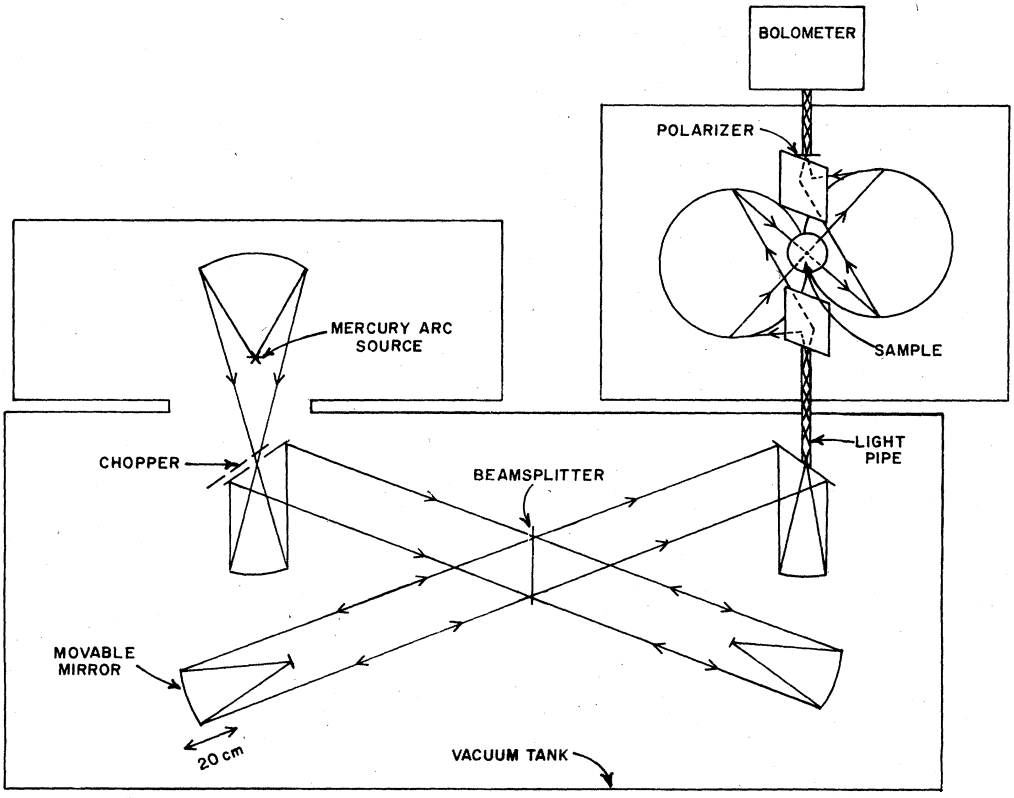

FIG. 3. Diagram of Michelson interferometer used to cover the 10—700 cm^{-1} region.

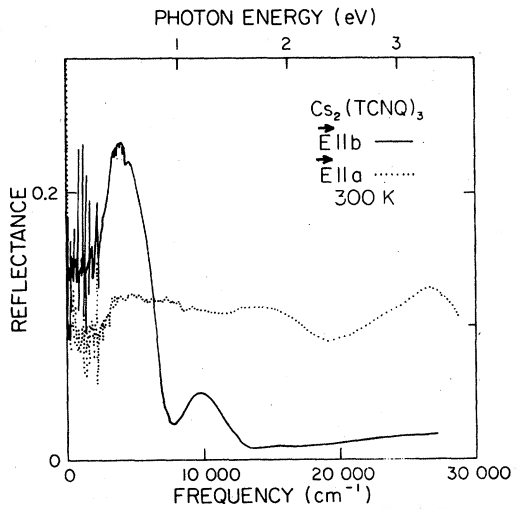

FIG. 4. Polarized reflectance of $Cs_2(TCNQ)_3$ at room temperature for $\vec{E}||a$ (dotted line) and $\vec{E}||b$ (solid line) between 10 and 30000 cm^{-1}.

from the mosaic with the reflectance of the same mosaic after coating with gold. By taking the ratio of these values an absolute measurement of the reflectance was obtained for the far infrared.

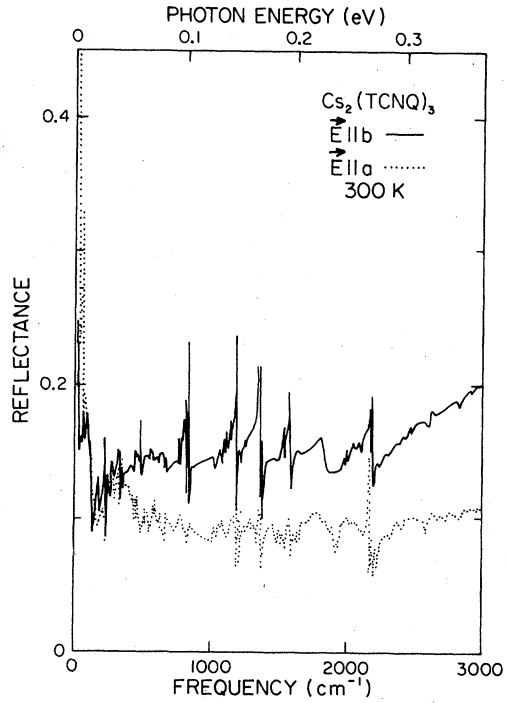

FIG. 5. Polarized reflectance data at low frequencies (10–3000 cm^{-1}).

III. EXPERIMENTAL RESULTS

The reflectance of $Cs_2(TCNQ)_3$ with $\vec{E}||b$ and $\vec{E}||a$ from the far infrared to the ultraviolet is shown in Fig. 4. Between 4000 and 30000 cm^{-1} (0.5–3.7 eV) there are two broad maxima in both polarizations. These maxima are associated with electronic transitions in the material. Figure 5 shows in detail the reflectance from 10 to 3000 cm^{-1} (0.001–0.04 eV). The sharp features in this region are associated with molecular vibrations. Notice the sharp low-frequency rise in the $\vec{E}||a$ component of the reflectance.

Because an extremely large frequency region was covered, a Kramers-Kronig analysis[24] of the reflectance should provide reasonably accurate values for the optical constants. In the perfomance of the analysis conventional extrapolation procedures were used. At very low frequencies the reflectance was assumed constant. Between the highest-frequency data point and 200000 cm^{-1} (25 eV) the reflectance was extrapolated as $1/\omega^2$ to simulate interband transitions while above 200000 cm^{-1} a $1/\omega^4$ form, appropriate for free-electron behavior, was used. The computer program determines the phase shift on reflection from the Kramers-Kronig integral. From the reflectance and phase all of the usual optical functions are calculated.

The frequency-dependent conductivity $\sigma_1(\omega)$ is given over the whole frequency region in Fig. 6; the low-frequency details are shown in Fig. 7. The energies of the maxima in $\sigma_1(\omega)$ give the energies of electronic or vibrational transitions in the solid more closely than the absorption coefficient α or the imaginary part of the dielectric function. Figure 6 shows quite clearly that the strengths of the electronic transitions in $\vec{E}||a$ are three to four times greater than those in $\vec{E}||b$. The small negative values of $\sigma_1(\omega)$ which occur near the strong structures at low frequencies arise because little apodization was used on the interferogram from the Michelson interferometer.

Figure 8 shows the real part of the dielectric function $\epsilon_1(\omega)$ on a logarithmic frequency scale. The dielectric function displays the usual derivativelike structure at frequencies near the conductivity maxima. Extrapolation of the infrared data to zero frequency gives a value of 5.0 ± 0.1 for the static dielectric constant.

IV. DISCUSSION

A. Electronic transitions

In this section we compare our experimental results with theoretical approaches appropriate for

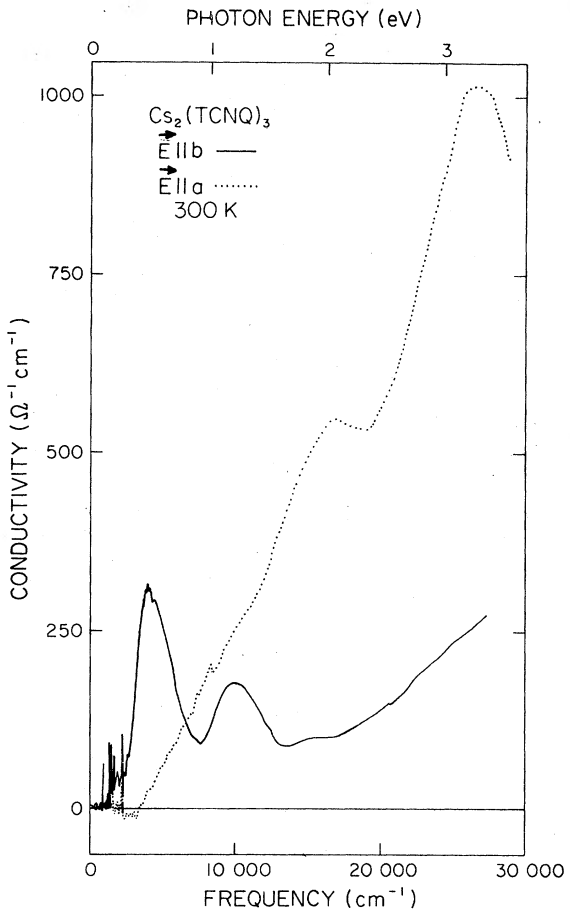

FIG. 6. Frequency-dependent conductivity obtained by Kramers-Kronig analysis of the reflectance for room temperature $Cs_2(TCNQ)_3$. The conductivity for $\vec{E}||a$ is shown as a dotted line while that for $\vec{E}||b$ is shown as a solid line.

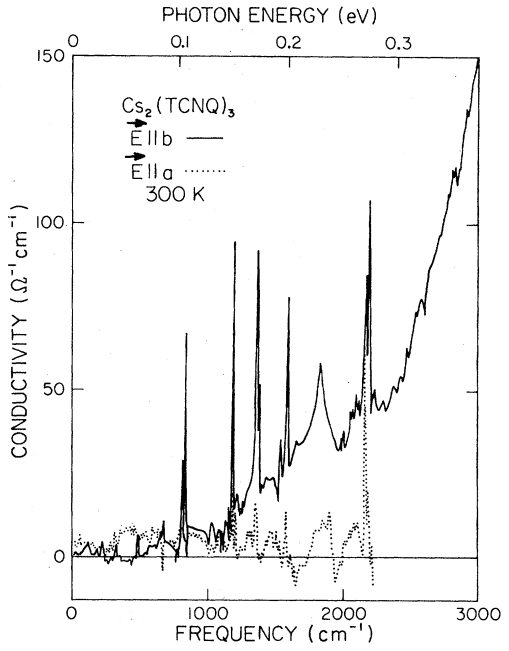

FIG. 7. Frequency-dependent conductivity at low frequencies.

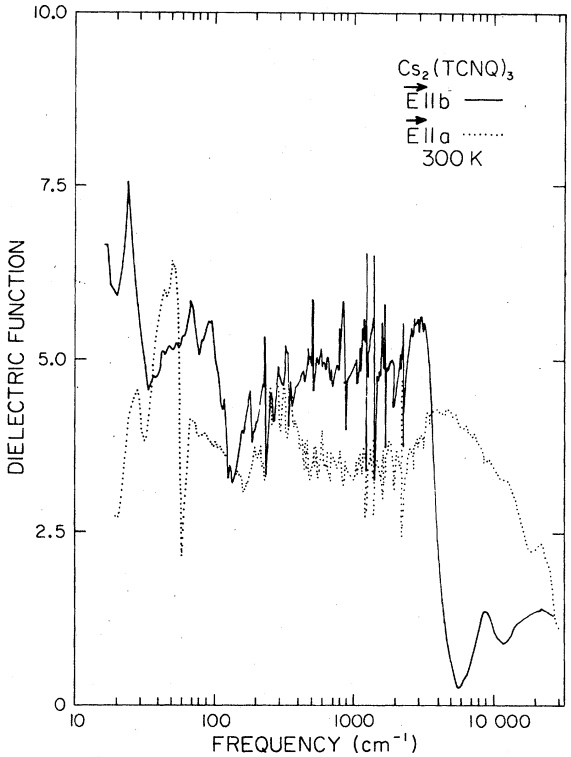

FIG. 8. Real part of the dielectric function obtained by Kramers-Kronig analysis of the reflectance for room temperature $Cs_2(TCNQ)_3$. Note that the figure has a logarithmic frequency scale.

$Cs_2(TCNQ)_3$. These theories all stress the importance of the Coulomb interaction for determining optical properties. This interaction is important because an electron transferred to an adjacent molecule has its energy raised by the Coulomb interaction with the electron on that and neighboring molecules. Implicit in these models is the assumption that the electrons are localized on individual molecular sites. Delocalization across many sites to form energy bands would make the Coulomb interaction of the electrons much less important.[11,21]

In a model proposed by Hubbard,[25] TCNQ charge-transfer salts are assumed to form a one-dimensional localized array of electrons. Because $Cs_2(TCNQ)_3$ has two valence electrons for every three molecules the array has two sites occupied by

electrons and then one site vacant. This model of $Cs_2(TCNQ)_3$ is strongly supported by the x-ray data,[1] which imply that two molecules are negative and one is neutral. With this arrangement there can be two charge-transfer transitions. The first is the transition of an electron to another already occupied site. We will call this charge-transfer excitation the "dimer" transition because it occurs within the dimers of negatively charged molecules. The second transition is that of an electron to a site which is unoccupied or a "neutral" transition. The dimer transition energy is determined by both on-site and off-site Coulomb interaction strengths while the neutral transition energy involves only the off-site terms. Hubbard calculated the on-site interaction energy from the disproportionation energy for the reaction $2TCNQ^- \rightarrow TCNQ + TCNQ$,[2-26] while the off-site energies were calculated from the electrostatic interaction of the charge distribution[26] on nth-neighbor TCNQ ions of the TCNQ chain. The off-site terms include only those neighbors within three lattice sites of the transition electron under consideration when calculating the energies of each configuration.

By calculating the Coulomb energy associated with the final state and subtracting the energy of the ground state we can estimate the energy for each transition. These energies are given in Table I. The values of on-site and off-site Coulomb interactions used were those given by Hubbard[25] with modification of the "screening by polarization" because the dielectric constant of $Cs_2(TCNQ)_3$ is less than the material (TTF-TCNQ) Hubbard discussed. The neutral transition is calculated to have an energy of $E_N = 1400$ cm^{-1} (0.17 eV). However, from Fig. 6 and Table I we find experimentally $E_N = 3900$ cm^{-1} (0.48 eV). It appears that Hubbard overestimated the value of the third-order off-site interaction energy. To reproduce accurately our experimental data, the value of the third-order term must be reduced to very near zero. The model predicts that the dimer transition should occur at $E_{CT} = 8000$ cm^{-1} (1.0 eV, approximately the value of U_{CT}; CT here means charge transfer), a frequency which is lower than the experimentally determined frequency of 9980 cm^{-1} (1.24 eV). As will be shown below, this discrepancy arises from the neglect of the transfer integral t in this model.

A theory for the dimer interaction has been described, in terms of the Hubbard model, by Harris and Lange[27] and elaborated by Rice.[28] This theory focuses specifically on the interaction within the dimer of the singly occupied π molecular orbitals of the two $TCNQ^-$ ions. The theory used as parameters the overlap matrix element or transfer integral t and the on-site Coulomb interaction U. The transfer integral represents the overlap of electronic wave functions within the dimer and the Coulomb interaction describes the net cost of having both electrons occupy the same molecular orbital.

When these interactions are considered, the original energy level of the monomer splits into four levels in the dimer. The ground state is a bonding arrangement with one electron on one molecule and the other electron, with opposite spin, on the

TABLE I. Electronic excitation energies in $Cs_2(TCNQ)_3$.

	Frequencies in cm^{-1}					
Elect. trans	Expt. data[a]	Rice Ref. 28	Hubbard Ref. 25	Tanaka Ref. 12 Theory (expt.)[d]	Previous experimental data note f	note g
Δ_x	751[b]	756		766[e]		
E_N	3872		1371(4436)[c]	5800(6000)	5500	3650
E_{CT}	9977	9970	8066	10 800(11 000)	10 600	11 600
E_{LE1}	16 411			17 200(17 700)	16 500	17 000
E_{LE2}	26 348			(30 000)	28 000	26 600

[a]Data obtained from conductivity, $\sigma_1(\omega)$ (this work).
[b]Data taken from Ref. 6 (751 cm^{-1} = 540 K).
[c]Recalculated with third-order interaction equal to zero.
[d]Calculated values are given with corresponding observed values in parentheses.
[e]One-half the value discussed by Ref. 12.
[f]Pressed powder unpolarized spectra from Refs. 7, 13, and 29.
[g]Pressed powder spectra with polarization determined by transmission from Ref. 11.

other molecule. The next level is a triplet state having one electron on each molecule but with parallel spins. This state is excitable magnetically from the ground state with energy

$$\Delta_x=(U^2/4+4t^2)^{1/2}-U/2\ . \tag{1}$$

Above the triplet level is a state where two electrons, with opposite spin, are localized on one of the two molecules. This "charge-transfer" state is coupled by the electric dipole operator to the ground state and is at an energy

$$E_{\rm CT}=U/2+(U^2/4+4t^2)^{1/2} \tag{2}$$

above the ground state. Finally, the highest level is an antibonding version of the ground state.

The optical charge-transfer excitation, polarized along the b axis joining the two molecules, occurs at $\omega_{\rm CT}=E_{\rm CT}/\hbar$. The dielectric tensor has been derived by Rice[28] and is given by

$$\epsilon(\vec{\vec{\omega}})=\vec{\vec{\epsilon}}_r+\frac{4\pi ne^2b^2}{\hbar^2}\times\vec{\vec{A}}\frac{4t^2/(U^2/4+4t^2)^{1/2}}{\omega_{\rm CT}^2[1-D(\omega)]-\omega^2-i\omega\gamma}\ . \tag{3}$$

In Eq. 3, $\vec{\vec{\epsilon}}_r$ includes the contribution of other excitations to the dielectric tensor, n is the density of molecules, b is the intradimer separation, γ is a phenomenological linewidth, and $D(\omega)$ is a function which describes the effects arising from the coupling of the unpaired electron to the internal vibrations of the TCNQ molecule. In the region of electronic transitions, however, $D(\omega)<<1$ so we can neglect this function here. The tensorial character comes from

$$\vec{\vec{A}}=(1/N)\sum_{j=1}^{N}\vec{a}_j\vec{a}_j/|a_j|^2$$

($\vec{a}_j$ is the vector joining the centers of the jth dimer and N is the number of dimers). For $Cs_2(TCNQ)_3$ $b=3.22$ Å and the diagonal component of $\vec{\vec{A}}$ along the b crystallographic axis is $A_{bb}=0.995$.[1] The charge-transfer band has an oscillator strength which can be obtained by integrating the conductivity $\sigma_1(\omega)$ over the charge-transfer band

$$\int_{\rm CT}\sigma_1(\omega)d\omega=\frac{\vec{\vec{A}}\pi ne^2b^2}{\hbar^2}\frac{2t^2}{(U^2/4+4t^2)^{1/2}}\ . \tag{4}$$

The oscillator strength then may be rewritten by using a partial conductivity sum rule[24]

$$S(\omega)=N_e\frac{m}{m^*}=\frac{2mV_a}{\pi e^2}\int_0^{\omega}\sigma_1(\omega')d\omega'\ . \tag{5}$$

In Eq. (5) m is the electronic mass, m^* is the effective mass of the conduction electrons, V_a is the volume per anion, and $N_e=nV_a$. The parameters t and U may be calculated from optical data on the frequency of the charge-transfer band [Eq. (2)] and its oscillator strength [Eqs. (4) and (5)].

The charge-transfer excitation is the second peak in the $\vec{E}||b$ conductivity at 9980 cm^{-1} (1.24 eV, Fig. 6). Figure 9 shows a partial sum rule $S(\omega)$ for $Cs_2(TCNQ)_3$. By subtracting the value of $S(17\,500\ cm^{-1})$ from $S(7700\ cm^{-1})$, Fig. 9 gives $(m/m^*)N_e=0.23$ for the dimer transition. Using these values in the dimer theory we obtain $U=1.14$ eV (9240 cm^{-1}) and $t=0.17$ eV (1350 cm^{-1}). The quantity $(m/m^*)N_e$ can also be calculated from the observed plasmon frequencies, using

$$\tilde{\omega}_{p2}^2-\tilde{\omega}_{p1}^2\simeq\frac{4\pi ne^2}{m^*\epsilon_\infty}\ , \tag{6}$$

where $\tilde{\omega}_p$ is the screened plasmon frequency for each transition and ϵ_∞ is the high-frequency dielectric constant. Figure 10 displays the electron-energy-loss function and shows that $\tilde{\omega}_{p1}=6620$ cm^{-1} and that $\tilde{\omega}_{p2}=11\,600\ cm^{-1}$. With $\epsilon_\infty=1.3$ from Fig. 8 we calculate $(m/m^*)N_e=0.22$ in close agreement with the earlier value.

The values for t and U are consistent with previously reported data on similar systems.[11–13,18,19,29,30] The agreement between these dimeric values of U and t and those obtained[18] for $D(CH_3)Fc$-TCNQ ($U=1.0$ eV and $t=0.27$ eV) is quite good. Since $D(CH_3))F_c$-TCNQ contains contain isolated dimers, this agreement lends confidence to our use of this model for the dimers in $Cs_2(TCNQ)_3$. In addition, Eq. (1) predicts the activation energy for the magnetic susceptibility. Using the values for U and t above we calculate an activation energy of 543 K. Experimentally $Cs_2(TCNQ)_3$ has an activation energy of 540 K (Ref. 6) in good agreement with this estimate. Table I shows a comparison between experimental data and the theories which are discussed here.

A third model which uses a modified Hubbard Hamiltonian has been described by Tanaka *et al.*[12] Three interactions are included in this model: the

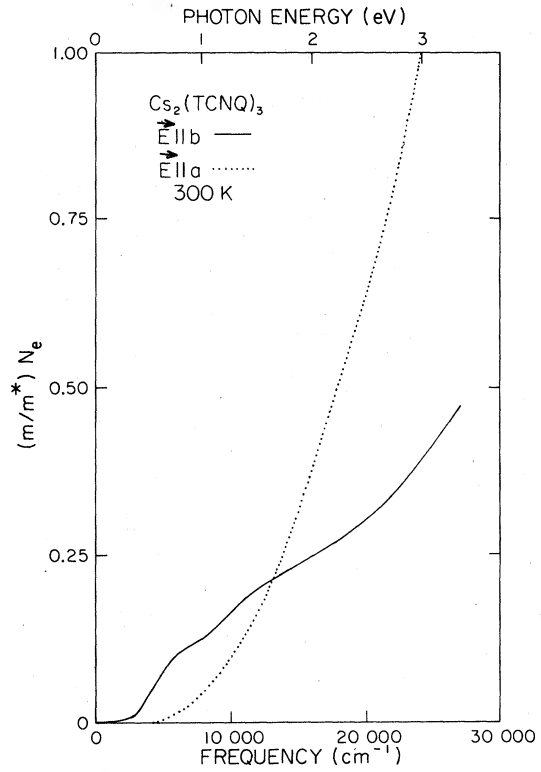

FIG. 9. Effective number of electrons determined by integration of the Kramers-Kronig derived conductivity.

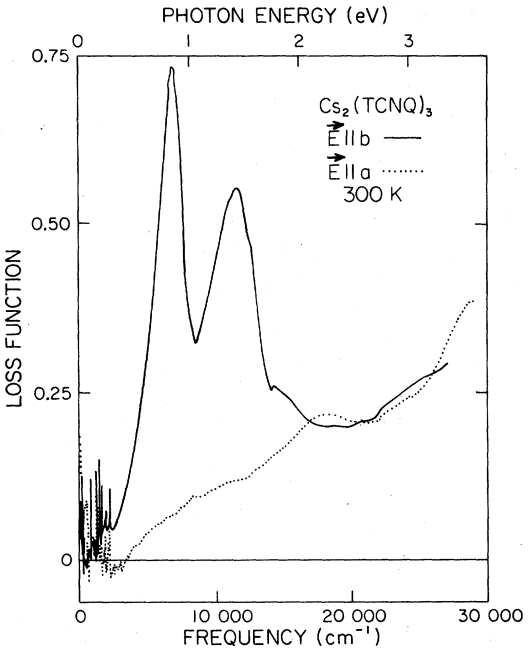

FIG. 10. Electron-energy-loss function obtained by Kramers-Kronig analysis of the reflectance, shown for $\vec{E}||a$ (dotted line) and $\vec{E}||b$ (solid line) between 10 and 30 000 cm^{-1}.

"dimer" charge transfer, the "neutral" charge transfer, and a "localized excitation" of an electron from a lower orbital in $TCNQ^-$ to an upper energy state. From numeric computations and fitting to their data they find $E_{CT}=10\,800$ cm^{-1} and $E_N=5800$ cm^{-1}. They find the transfer integral $t=0.27$ eV and estimate $U=1.5$ eV for $Cs_2(TCNQ)_3$. These values are consistently higher when compared to our results of $t=0.17$ eV and $U=1.14$ eV (see Table I). It is clear that the discrepancy arises because they fit their theory to the absorption coefficient, which tends to peak at higher frequencies than the corresponding structure in the conductivity.

The third transition of an electron excited to a higher orbital or localized excitation was shown to be polarized along the a axis with an energy $E_{LE1}=17\,200$ cm^{-1}. In Fig. 6 the energy of the first localized excitation appears as the peak in the $\vec{E}||a$ conductivity at $E_{LE1}=16\,400$ cm^{-1} (2.0 eV). A second localized excitation occurs at $E_{LE2}=26\,350$ cm^{-1} (3.3 eV). Again Tanaka *et al.*[12] have consistently higher values for excitation energies.

To make a final comparison between experiment and theory we note that the one-dimensional Hubbard model has been solved exactly at $T=0$ K by Lieb and Wu.[31] They find that for $t>>U$ the electrons delocalize into a single conduction band but for $t<<U$ the electrons remain localized on particular molecules forming a semiconductor in the half-filled-band case. The minimum band gap in this semiconductor is

$$E_g \simeq U-4t\ . \tag{7}$$

By using the values of U and t obtained from the dimer transition, we find $E_g=0.46$ eV. This value is not in very good agreement with the experimental results of Blakemore *et al.*,[5] who obtain $E_g=0.72$ eV for $Cs_2(TCNQ)_3$ using dc conductivity measurements. Interestingly, the gap obtained from dc conductivity falls almost exactly between the two transitions observed in $\vec{E}||b$.

According to Tanaka *et al*,[12] somewhat better results can be obtained if the transfer integral is calculated for the neutral transition and then t is averaged over the nearest neighbors. Using their values in the calculation we obtain $E_g=0.90$ eV. Only when third-neighbor terms are included in the average of the transfer integral t does the estimate [Eq. (7)] of the activation energy begin to

predict the experimental value.

If we compare the results from $Cs_2(TCNQ)_3$ with another TCNQ system that has $\frac{2}{3}$ of an electron per molecule in its unit cell, $N(CH_3)_3H$-I-TCNQ,[21,32,33] we notice the electronic spectra are quite different. Neither the neutral nor dimer transition occurs in the spectra of $N(CH_3)_3H$-I-TCNQ. Instead, a single low-lying peak is observed, centered at 1600 cm^{-1}. In $Cs_2(TCNQ)_3$ the Coulomb interactions are strong and therefore the electrons are assumed to be localized, while in $N(CH_3)_3H$-I-TCNQ the electrons are assumed to be uniformly distributed causing it to be a semiconductor with an energy gap of approximately 0.17 eV. Comparison between these two compounds indicates to us that electronic structure of TCNQ compounds is not determined simply by charge transfer and Coulomb interactions but instead is controlled by crystal structure or by other interactions.

B. Vibrational modes

A series of strong, narrow infrared absorption bands in $Cs_2(TCNQ)_3$ is shown in Figs. 5 and 7. As discussed by Rice,[28] some of these bands appear for a dimer on account of electron-molecular-vibration coupling. In nondimerized TCNQ the totally symmetric (a_g) molecular vibration modes, having no dipole moment, are optically inactive. In a dimer, however, the antisymmetric combinations of these a_g modes couple directly to the dimer charge-transfer excitations and therefore drive oscillations in the radical electrons electric dipole moment. These "dimer charge oscillations" give infrared activity to the a_g modes polarized in the direction of the dimer axis. The oscillations are described by $D(\omega)$ in Eq. (3) where

$$D(\omega)=\sum_{\alpha=1}^{G}\frac{\lambda_\alpha\omega_\alpha^2}{\omega_\alpha^2-\omega^2-i\omega\gamma_\alpha}\ . \tag{8}$$

In Eq. (8), G is the number of modes, ω_α is the "bare" frequency of the αth a_g mode, γ_α is the linewidth of the mode, and λ_α is a dimensionless constant which indicates the strength of the dimer charge transfer-molecule-vibration coupling:

$$\lambda_\alpha=\frac{16t^2}{(\hbar\omega_{CT})^2(U^2/4+4t^2)^{1/2}}\frac{g_\alpha^2}{\hbar\omega_\alpha}\ , \tag{9}$$

where g_α is the a_g electron-molecular-vibration coupling constant for mode α. (Typically, $\lambda_\alpha\sim10^{-2}$.) These equations can be used to obtain "experimental" values for the parameters ω_α, g_α, and γ_α. Before a fit can be done, however, the many modes seen in Fig. 7 must be assigned.

When reviewing the papers of previous workers that have assigned vibrational modes to the optical spectra of $TCNQ^-$, one gets a confusing picture because many earlier workers did not assign a_g modes to dimeric forms of TCNQ. The assignment of modes in the case of $Cs_2(TCNQ)_3$ is further complicated by the fact that both $TCNQ^0$ and $TCNQ^-$ are present in the spectra.

In Table II, we present an assignment of the observed vibrational modes of $Cs_2(TCNQ)_3$. The first three columns give the symmetry species, the vibrational mode (following the notation of Girlando and Pecile[34]), and our observed frequencies. The next column gives theoretical estimates for the frequencies, while the last two columns list observed frequencies in the neutral molecule[34] and in the radical anion.[35] A recent calculation of the normal modes of $TCNQ^0$ and $TCNQ^-$ by Khatkale and Devlin[36] differs only slightly from the frequencies in Table II. Some of the expected frequencies for the vibrations of the neutral molecule and the radical ion are so close that they cannot be separated in our data. In addition, many of the modes associated with the $TCNQ^0$ molecule do not appear in our spectra. None of the b_{1u} neutral molecule vibrations were identified, while low-frequency modes (below $b_{2u}\nu_{36}^0$ and $b_{3u}\nu_{50}^0$) were probably too weak to be seen in the reflectance. Those features which have not been seen previously (e.g., $b_{2u}\nu_{36}^0$, ν_{37}^-, ν_{39}^-, and ν_{40}^-) were assigned on the basis of the calculated frequency and the expected polarization dependence of each symmetry species. The relative strength of each symmetry species in $Cs_2(TCNQ)_3$ for all three polarizations is given in Table III. The modes of the ion are twice as strong as those of the neutral molecule. Notice in Fig. 7 that b_{2u} modes only appear in $\vec{E}||a$ polarization and b_{3u} modes are only seen for $\vec{E}||b$, while b_{1u} modes are seen in both polarizations. The $b_{1u}\nu_{26}^-$ and $b_{2u}\nu_{36}^0$ modes are very weak in our spectrum and therefore have the greatest uncertainty. Several weak modes between 700 and 1000 cm^{-1} are not observed because of a poor signal-to-noise ratio in our instrumental overlap region. Most of our remaining assignments follow previous work[14,34–38] with very little change. The a_g modes appear in both polarizations but, of course, occur only for the $TCNQ^-$

TABLE II. Observed vibrational frequencies in $Cs_2(TCNQ)_3$.

Symmetry species	Vibrational[a] mode	Frequencies in cm^{-1} $Cs_2(TCNQ)_3$[b] Freq.	Intensity	Calculation[c]	Other TCNQ compounds[d] ($TCNQ^0$) (Ref. 34)	($TCNQ^-$) (Ref. 35)
a_g	ν_2^-	2184	vs	2186		2206
	ν_3^-	1585	vs	1589		1615
	ν_4^-	1360	vs	1403		1391
	ν_5^-	1185	vs	1206		1196
	ν_8^-	607	w	607		613
	ν_9^-	325	s	337		337
	ν_{10}^-	119	m	126		148
b_{1u}	ν_{19}^-	2166	vs	2186		2181
	ν_{20}^-	1538	s	1514		1504
	ν_{21}^-	1370	s	1386		1361
	ν_{25}^{0-}	528	vw	524	549	541
	ν_{26}^{0-}	152	vw	160	146	
b_{2u}	ν_{33}^0	2217	w	2226	2228	
	ν_{34}^0	1535	m	1530	1540	
	ν_{34}^-	1507	m	1525		1518
	ν_{35}^-	1353	m	1390		1388
	ν_{35}^0	1328	w	1360	1354	
	ν_{36}^-	1211	s	1221		1210
	ν_{36}^0	1203	vw	1209		
	ν_{37}^-	1131	w	1133		
	ν_{38}^{0-}	478	vw	505	498	512
	ν_{39}^{0-}	283	m	297		
	ν_{40}^{0-}	54	m	60		
b_{3u}	ν_{50}^-	830	s			836
	ν_{50}^0	813	s		859	
	ν_{51}^-	571	w			585
	ν_{52}^{0-}	485	m		475	483
	ν_{53}^{0-}	222	m		220	225
	ν_{54}^{0-}	107	m		103	

[a] $\nu_N^{0-} \rightarrow$ could not distinguish between $TCNQ^0$ and $TCNQ^-$ modes.
[b] Data from $\sigma_1(\omega)$ (this work).
[c] $TCNQ^0$ calculations taken from Ref. 34 and $TCNQ^-$ calculations taken from Ref. 35.
[d] Observed frequencies. Line indicates mode was not observed. vs = very strong, s = strong, m = medium, w = weak, and vw = very weak.

TABLE III. Calculated relative strength of vibrational modes.

Mode	$\vec{E}\|\|a$	$\vec{E}\|\|b$	$\vec{E}\|\|c$
b_{1u}^0	0.25	0.33	0.43
b_{1u}^-	0.60	0.62	0.80
b_{2u}^0	0.96	0.00	0.02
b_{2u}^-	1.96	0.00	0.04
b_{3u}^0	0.01	0.50	0.48
b_{3u}^-	0.02	1.22	0.78

ion.

After assigning the a_g features in our data, we have fit the dimer charge oscillation of Rice,[28] Eqs. (3), (8), and (9), to the data. A nonlinear least-squares fit[39] to the $\vec{E}||b$ conductivity was used to extract the parameters for each a_g mode. Unfortunately, our data between 700 and 1000 cm^{-1} were not of sufficient quality to observe the a_g modes in this region.

Figure 11 shows the conductivity data and the fit to this data. The paraboliclike background was

TABLE IV. Electron-molecular-vibration coupling parameters for $Cs_2(TCNQ)_3$.

Mode	Unperturbed frequencies ω_α in cm^{-1}				Coupling strengths g_α in meV				
	$Cs_2(TCNQ)_3$[a]	$D(CH_3)Fc$-TCNQ (Ref. 18)	K-TCNQ (Refs. 19 and 20)	MEM-TCNQ (Ref. 30)	Theory (Ref. 36)	$Cs_2(TCNQ)_3$[a]	$D(CH_3)Fc$-TCNQ (Ref. 18)	K-TCNQ (Refs. 19 and 20)	MEM-TCNQ (Ref. 30)	Theory (Refs. 20, 40, and 41)
$a_g\nu_2^-$	2192	2214	2225	2210	2195	64	101	73	43	52
$a_g\nu_3^-$	1598	1610	1632	1630	1595	89	67	83	67	131
$a_g\nu_4^-$	1380	1398	1395	1395	1368	106	86	71	62	49
$a_g\nu_5^-$	1197	1186	1206	1180	1202	71	43	41	37	28
$a_g\nu_8^-$	610		485	597	606	<10		23	6	2
$a_g\nu_9^-$	328		333	324	319	30		22	22	24
$a_g\nu_{10}^-$	136			150	142	106			9	10

[a]Data from this work.

simulated by using a complex frequency-dependent dielectric function for the high-frequency background ϵ_r. The fitting procedure gave values between 4 and 25 cm^{-1} for the γ_α. The values for the unperturbed frequencies ω_α and the electron-molecular-vibration coupling constants g_α are given in Table IV. Table IV also summarizes other experimental[18,20,30] and theoretical[40,41] values for these parameters. Notice that the calculated frequency is always higher than the observed frequency in the conductivity (i.e., the effect of the coupling to the electron is to lower the frequency of the mode). The values obtained for g_α are in general agreement with both theoretical and observed values in a variety of TCNQ systems. However, the values of g_4, g_5, and g_{10} considerably exceed the values expected from theory. It is suspected that the large value for g_{10} along with the large γ_{10} may be caused by a problem with an overlapping structure in the reflectance spectrum. The observed frequencies for the modes are consistent for each material and we note that many of the very strong modes in the $\vec{E}||b$ conductivity arise from the dimer charge oscillations.

In summary, by measuring the optical properties of $Cs_2(TCNQ)_3$, we have examined electronic ener-

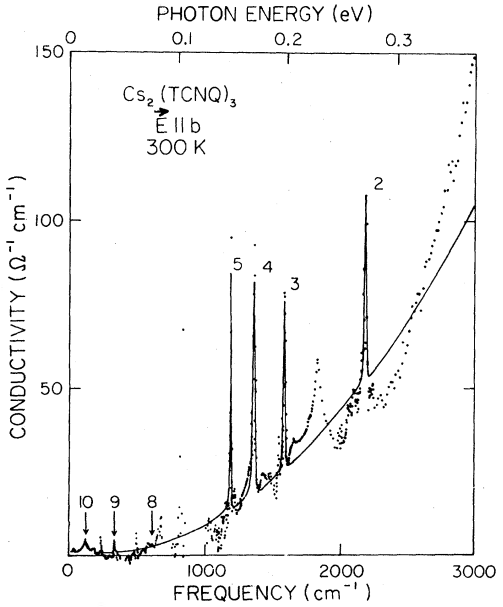

FIG. 11. Frequency-dependent conductivity for $Cs_2(TCNQ)_3$ (10–3000 cm^{-1}). The points represent the data for $\vec{E}||b$ and a fit of the theory of electron-molecular-vibration coupling in the dimer to the data is shown as the solid line. The numbers correspond to the assigned a_g modes of the $TCNQ^-$ molecule.

gies and electron-molecular-vibration coupling in this material. Five interactions have been investigated in this organic crystal: the transfer matrix element (t), the on-site Coulomb repulsion (U), the off-site or neighboring Coulomb interactions, the interaction energy between charge-transfer and localized excitations, and the electron-phonon coupling constants (g_a). From analysis of the dimer charge-transfer excitation we obtain the values $U=1.4$ eV and $t=0.17$ eV. If these values are applied to linear-chain TCNQ systems, then the bandwidth would be $W=4t=0.7$ eV $<U$. Since $U>4t$ the Coulomb interactions are strong and the picture of localized electrons used to describe $Cs_2(TCNQ)_3$ is valid.

By extending the optical work below 500 cm^{-1} on $Cs_2(TCNQ)_3$, we have been able to examine more modes of vibration in the $TCNQ^0$ molecule and $TCNQ^-$ ion. From analysis of the a_g modes, values for the electron-phonon coupling constants were obtained. We have also attempted to clarify some of the confusion which exists in the literature by systematically assigning vibrational modes of $TCNQ^0$ and $TCNQ^-$ in the optical spectra.

ACKNOWLEDGMENT

We thank M. J. Rice for several useful discussions.

[1]C. J. Fritchie, Jr. and P. Arthur, Jr., Acta. Crystallogr. 21, 139 (1966).
[2]W. J. Siemons, P. E. Bierstedt, and R. G. Kepler, J. Chem. Phys. 39, 3523 (1963).
[3]J. G. Vegter, T. Hibma, and J. Kommandeur, Chem. Phys. Lett. 3, 427 (1969).
[4]N. Sakai, I. Shirotani, and S. Minomura, Bull. Chem. Soc. Jpn. 45, 3314 (1972).
[5]J. S. Blakemore, J. E. Lane, and D. A. Woodbury, Phys. Rev. B 18, 6797 (1978).
[6]J. Vegter, J. Kommandeur, and P. Fedders, Phys. Rev. B 7, 2929 (1973).
[7]Y. Iida, Bull. Chem. Soc. Jpn. 42, 637 (1969).
[8]S. Hiroma, H. Kuroda, and H. Akamatu, Bull. Chem. Soc. Jpn. 44, 9 (1971).
[9]R. M. Vlasova and A. I. Gutman, Fiz. Tverd. Tela (Leningrad) 13, 2808 (1971) [Sov. Phys.—Solid State 13, 2356 (1972)].
[10]Y. Oohashi and T. Sakata, Bull. Chem. Soc. Jpn. 48, 1725 (1975).
[11]J. B. Torrance, B. A. Scott, and F. B. Kaufman, Solid State Commun. 17, 1369 (1975).
[12]J. Tanaka, M. Tanaka, T. Kawai, T. Takabe, and O. Maki, Bull. Chem. Soc. Jpn. 49, 2358 (1976).
[13]Y. Iida, Bull. Chem. Soc. Jpn. 51, 434 (1978).
[14]M. V. Belousov, A. M. Vainrub, R. M. Vlasova, and V. N. Semkin, Fiz. Tverd. Tela (Leningrad) 20, 107 (1978) [Sov. Phys.—Solid State 20, 58 (1978)].
[15]T. Kondow and T. Sakata, Phys. Status Solidi 6, 551 (1971).
[16]A. Girlando, R. Bozio, and C. Pecile, Chem. Phys. Lett. 25, 409 (1974).
[17]S. M. Khursandova, R. M. Vlasova, L. P. Rautian, V. N. Semkin, A. A. Berlin, A. I. Sherle, and M. I. Cherkashin, Fiz. Tverd. Tela (Leningrad) 20, 3542 (1978) [Sov. Phys.—Solid State 20, 2049 (1978)].
[18]D. B. Tanner, J. S. Miller, M. J. Rice, and J. J. Ritsko, Phys. Rev. B 21, 5835 (1980).
[19]D. B. Tanner, C. S. Jacobsen, A. A. Bright, and A. J. Heeger, Phys. Rev. B 16, 3283 (1977).
[20]M. J. Rice, N. O. Lipari, and S. Strassler, Phys. Rev. Lett. 39, 1359 (1977).
[21]D. B. Tanner, J. E. Deis, A. J. Epstein, and J. S. Miller, Solid State Commun. 31, 671 (1979).
[22]L. R. Melby, R. J. Harder, W. R. Nertler, W. Mahler, R. E. Benson, and W. E. Mochel, J. Am. Chem. Soc. 84, 3374 (1962).
[23]R. B. Sanderson and H. E. Scott, Appl. Opt. 10, 1097 (1971).
[24]Fredwick Wooten, *Optical Properties of Solids* (Academic, New York, 1972).
[25]J. Hubbard, Phys. Rev. B 17, 494 (1978).
[26]H. Johansen, Int. J. Quantum Chem. 9, 459 (1975).
[27]A. B. Harris and R. V. Lange, Phys. Rev. 157, 295 (1967).
[28]M. J. Rice, Solid State Commun. 31, 93 (1979).
[29]J. Vegter and J. Kommandeur, Phys. Rev. B 9, 5150 (1974).
[30]M. J. Rice, V. M. Yartsev, and C. S. Jacobsen, Phys. Rev. B 21, 3437 (1980).
[31]E. H. Lieb and F. Y. Wu, Phys. Rev. Lett. 20, 1445 (1963).
[32]D. B. Tanner, in *Extend Linear Chain Compounds*, edited by Joel S. Miller (Plenum, New York, 1981), Vol. 2, p. 205.
[33]D. B. Tanner, D. M. Hoffman, A. J. Epstein, and J. S. Miller (unpublished).
[34]A. Girlando and C. Pecile, Spectrochim. Acta Part A 29, 1859 (1973).
[35]R. Bozio, I. Zanon, A. Girlando, and C. Pecile, J. Chem. Soc. Faraday Trans. 1 74, 235 (1978).
[36]M. S. Khatkale and J. P. Devlin, J. Chem. Phys. 70, 1851 (1979).
[37]T. Takenaka, Spectrochim. Acta Part A 27, 1735 (1971).
[38]R. Bozio, A. Girlando, and C. Pecile, J. Chem. Soc.

Faraday Trans. 1 71, 1237 (1975).
[39]Philip R. Bevington, *Data Reduction and Error Analysis for Physical Sciences* (McGraw-Hill, New York, 1969), Chap. 11.
[40]N. O. Lipari, C. B. Duke, R. Bozio, A. Girlando, C. Pecile, and A. Padva, Chem. Phys. Lett. 44, 236 (1976).
[41]M. J. Rice, C. B. Duke, and N. O. Lipari, Solid State Commun. 17, 1089 (1975).